Asociación Argentina
de Mecánica Computacional

Mecánica Computacional Vol XXX, págs. 1955-1975 (artículo completo)
Oscar Möller, Javier W. Signorelli, Mario A. Storti (Eds.)
Rosario, Argentina, 1-4 Noviembre 2011

AN INTRODUCTION TO ISOGEOMETRIC ANALYSIS APPLIED TO SOLID MECHANICS

Luis F. R. Espath[a], Alexandre L. Braun[b] and Armando M. Awruch[b]

[a]*Graduate Student PPGEC/UFRGS espath@gmail.com*

[b]*Graduate Program in Civil Engineering (PPGEC), Federal University of Rio Grande do Sul (UFRGS), Av. Osvaldo Aranha, 99, 3o andar, 90035-190, Porto Alegre, RS, Brazil, allbraun@ig.com.br, amawruch@ufrgs.br, http://www6.ufrgs.br/engcivil/*

Keywords: Isogeometric Analysis, NURBS, Corotational Kinematics, Solid Mechanics.

Abstract. The basic concepts related to Isogeometric Analysis applied to Solid Mechanics are introduced in this paper. Isogeometric Analysis is mainly concerned with exact discretization of the spatial field by using the same technologies adopted in Computer Aided Design (CAD) for the computational representation of geometric entities, which are also utilized to approximate the solution field. In addition, the method preserves the same framework employed by numerical models based on the Finite Element Method (FEM). In the present work, fundamental aspects on computational representation of geometric entities using B-*Splines* are briefly reviewed as a background for the introduction of Non Uniform Rational B-*Splines* (NURBS). A numerical model for linear and geometrically nonlinear Elasticity is formulated using the Bubnov-Galerkin weighted residual method and the isoparametric approach, where a corrotational formulation is adopted for the kinematical description of the motion. Element assembly procedures and evaluation of the stiffness matrix and load vector at local and global levels are described utilizing analogies with the FEM. Gauss quadrature is adopted for numerical integration of element matrices and relations among physical, parametric and parent fields are established. Classical examples are analyzed using NURBS and the displacement formulation. Results obtained with the present model are compared to benchmark predictions obtained from numerical schemes based on the FEM.

1 INTRODUCTION

Isogeometric analysis is devoted to unify numerical procedures related to geometrical design and analysis by using a single framework where the same techniques are utilized in both procedures. These tasks have been made independently with pre-processing programs based on CAD technologies and numerical solvers based on the FEM. Pre-processing includes CAD representation of physical prototypes, where a virtual model is obtained through a geometric translation from the actual model. In addition, meshing and imposition of boundary conditions and loads are also performed at this stage. However, it is observed that the finite element grid obtained after the mesh generation is only an approximation of the CAD geometrical model and poor approximations may be observed depending on the basis functions adopted during the spatial discretization. Hence, meshing procedures for finite element analysis usually deteriorate the CAD geometry, which is taken as "exact" when compared to the actual geometrical model.

The first step of a numerical analysis refers to the computational reproduction of a representative geometrical model using CAD technologies, which are also responsible for producing mesh information to be utilized in a finite element analysis. Although many technologies may be employed to represent general geometries computationally, one can observe that most of the commercial programs based on CAD adopts Non Uniform Rational B-*Splines* (NURBS) as a basic tool. NURBS are very useful since they can exactly represent all conics such as circles, ellipses, parabolas and hyperbolas.

An analysis procedure based on CAD formulation is referred to as Isogeometric Analysis. Isogeometric analysis offers the possibility of integrating Finite Element Analysis (FEA) with CAD tools by using B-*Splines* and NURBS parameterizations. Another important aspect related to Isogeometric Analysis is associated to the isoparametric concept, since the solution space is represented with the same basis functions utilized to represent the geometry. The general concepts on Isogeometric Analysis were first introduced by Elguedj et al. (2005) and simulations have been carried out, where very good results are observed for several applications in the field of solid and fluid mechanics, including structural vibrations, structural problems with small and large deformations and turbulent flows (see, for instance, Cottrell et al. (2006); Bazilevs et al. (2007); Elguedj et al. (2008)). A comprehensive work on Isogeometric Analysis may be found in Cottrell et al. (2009).

In the present work, a numerical model based on the Isogeometric Analysis is presented. General concepts on computational representation of geometric entities are briefly reviewed as a background for the introduction of Non Uniform Rational B-*Splines* (NURBS). Basic parameters such as knot vectors, control points and basis functions are also defined. An algorithm for linear and geometrically nonlinear Elasticity is developed using the Bubnov-Galerkin weighted residual method and the isoparametric approach applied on the equilibrium equation. Assembly and evaluation of the stiffness matrix and load vector at local and global levels are described utilizing analogies with the FEM. Gauss quadrature is utilized for numerical integration of element matrices and relations among physical, parametric and parent fields are established. In order to verify the present formulation with respect to important computational aspects such as accuracy and efficiency, comparisons are performed considering results obtained here for classical Elasticity applications and the corresponding predictions obtained from a numerical scheme based on a finite element model using eight-node hexahedrals with one-point quadrature, where benchmark results are also provided. All examples are modeled with NURBS surfaces and solids and the displacement formulation is adopted for the equilibrium description.

2 THEORETICAL ASPECTS

A set of statements referred to NURBS, Isogeometric Analysis, Corotational Kinematics and Solid Mechanics are presented in the following.

2.1 Fundamental concepts on CAD representation

There are three forms to represent a function: explicit, implicit and parametric form, where the explicit form is a particular case of an implicit form. The implicit form describes an implicit relation between the involved quantities. In parametric form, each quantities is explicitly and independently described as a function of parameters.

In order to describe complex curves, surfaces or solids, parametric representations are used. NURBS parameterization is well suitable to describe physical domains. In this sense, they can be used to describe the solution field. For beam, shell and solid brick structures, a curve representation in the form

$$\mathbf{C}(\xi) = (x(\xi), y(\xi), z(\xi)) \qquad (\xi) \in [0,1] \tag{1}$$

a surface representation in the form

$$\mathbf{S}(\xi,\eta) = (x(\xi,\eta), y(\xi,\eta), z(\xi,\eta)) \qquad (\xi,\eta) \in [0,1]\times[0,1] \tag{2}$$

a solid representation in the form

$$\mathbf{G}(\xi,\eta,\zeta) = (x(\xi,\eta,\zeta), y(\xi,\eta,\zeta), z(\xi,\eta,\zeta)) \qquad (\xi,\eta,\zeta) \in [0,1]\times[0,1]\times[0,1] \tag{3}$$

are looked for, respectively.

Computational modeling of geometric entities may be easily performed using polynomials as a basic tool. Polynomials are very useful since they can approximate a large number of functions. In addition, they can be easily differentiated and integrated.

A specific form to represent any given function is obtained by using Bernstein polynomials (Bernstein, 1912), where the Bernstein basis can be identified. A general formulation for Bernstein polynomials associated to a given degree n is defined as

$$B_{i,n}(\xi) = \binom{n}{i}\frac{(\xi-a)^i (b-\xi)^{n-i}}{(b-a)^n}, \quad \text{with} \quad \binom{n}{i} = \frac{n!}{i!\,(n-i)!} \tag{4}$$

where the parameter ξ of Bernstein bases must be defined over an interval, i.e., $\xi \in [a,b]$. For mathematical convenience, it is usually considered that $B_{i,n}(\xi) \stackrel{\text{def}}{=} 0$ if $i<0$ or $i>n$.

Bernstein polynomials, restricted to interval $[0,1]$, are utilized to form Bézier curves (Bézier, 1966, 1967, 1972). Considering that restriction, the Bernstein polynomials corresponding to degree n must be rewritten as follows:

$$B_{i,n}(\xi) = \binom{n}{i}\xi^i (1-\xi)^{n-i} \tag{5}$$

A recursive definition of Bernstein polynomials is obtained observing that they can be also defined by blending together two Bernstein polynomials of degree $n-1$, that is

$$B_{i,n}(\xi) = (1-\xi)B_{i,n-1}(\xi) + \xi B_{i-1,n-1}(\xi) \tag{6}$$

The most important properties associated to Bernstein polynomials are concerned to satisfying symmetry with respect to $\xi = \frac{1}{2}$, nonnegativity and partition of unity, which may be represented with the following expressions:

$$B_{i,n}(\xi) = (1-\xi)\, B_{n-i,n}(\xi) \qquad B_{i,n}(\xi) \geqslant 0 \qquad \sum_{i=0}^{n} B_{i,n}(\xi) = 1 \tag{7}$$

In order to obtain a stable numerical scheme to evaluate polynomials in Bernstein form, DeCasteljau's algorithm is usually employed (see Piegl and Tiller (1997); DeCasteljau (1959)).

A parametric formulation was introduced by Bézier (1966, 1967, 1972) to describe curves employing Bernstein polynomials, which are referred as being Bézier curves. A Bézier curve of degree n may be written as follows

$$\mathbf{C}(\xi) = \sum_{i=0}^{n} B_{i,n}(\xi)\, \mathbf{P}_i \qquad (\xi) \in [0,1] \tag{8}$$

where $\mathbf{P}_i$ are geometrical parameters (coordinates) defining the geometry in the physical space, which are known as control points, and $B_{i,n}(\xi)$ are Bernstein polynomials of degree n given as functions of variable ξ in the parametric space. The polygon defined with the control point is referred as being the control polygon (see Figures 1 and 2).

The Bézier parameterization to describe curves can be extended to surfaces by using the tensor product concept. The basis functions are now given as bivariate functions of parametric variables ξ and η, which are obtained from the product of univariate basis functions of degree n and m, respectively. In addition, a bidirectional grid of control points with dimensions $(n+1)\cdot(m+1)$ must be also specified. Consequently, a Bézier surface is obtained taking into account a bidirectional grid of control points, $\mathbf{P}_{i,j}$, and the product of Bernstein univariate polynomials, that is:

$$\mathbf{S}(\xi,\eta) = \sum_{i=0}^{n}\sum_{j=0}^{m} B_{i,n}(\xi)\, B_{j,m}(\eta)\, \mathbf{P}_{i,j} \qquad (\xi,\eta) \in [0,1] \tag{9}$$

In order to obtain a Bézier solid, the tensor product of univariate basis functions is employed to generate trivariate functions of parametric variables ξ, η and ζ of degree n, m and l, respectively. Considering a three-directional grid of control points, $\mathbf{P}_{i,j,k}$, with dimensions $(n+1)\cdot(m+1)\cdot(l+1)$, and the product of Bernstein univariate polynomials, as follows:

$$\mathbf{G}(\xi,\eta,\zeta) = \sum_{i=0}^{n}\sum_{j=0}^{m}\sum_{k=0}^{l} B_{i,n}(\xi)\, B_{j,m}(\eta)\, B_{k,l}(\zeta)\, \mathbf{P}_{i,j,k} \qquad (\xi,\eta,\zeta) \in [0,1] \tag{10}$$

Nevertheless, it is well known that complex geometric entities cannot be represented using just one polynomial function. Therefore, polynomials by parts have been employed to describe curves, surfaces and solids, where continuity at the breakpoints is enforced up to some desired order, which define the end points for every subdomain. These breakpoints are related to the knot vectors of the respective curve, surface or solid, in each direction. In this sense, B-*spline* geometries were introduced considering a linear combination of B-*spline* basis functions presenting minimal support with respect to a given degree, smoothness and domain partition.

The Cox-deBoor recursive formulation (Cox, 1972; deBoor, 1972) is usually adopted to evaluate B-*spline* basis functions, which are obtained considering a given knot vector $(\Xi, \mathcal{H}, \mathcal{Z})$,

which are defined over the parametric space, the number of control points $(n+1, m+1, l+1)$ and the polynomial degree (p, q, r), over the respective directions of the parametric space ξ, η and ζ.

The knot vector is a set of numerical values describing the knot coordinates in the parametric space, where a nonmonotonic sequence of increasing values must be chosen. Depending on the geometric topology, knot spans may represent points, lines or surfaces. After the knot coordinates are established, the knot spans are then defined and the extent of control of the control points over the geometry is also determined. Knots spans are always bounded by two consecutive knots, constituting the basic entities for Isogeometric Analysis in the same manner as elements are basic entities for Finite Element Analysis (FEA). Hence, the knot spans are also referred to as elements in Isogeometric Analysis.

The B-*spline* basis functions, in recursive form, are defined as:

$$\begin{aligned} N_{i,0}(\xi) &= \begin{cases} 1 & \text{if} \quad \xi_i \leqslant \xi < \xi_{i+1} \\ 0 & \text{otherwise} \end{cases} \\ N_{i,p}(\xi) &= \frac{\xi - \xi_i}{\xi_{i+p} - \xi_i} N_{i,p-1}(\xi) + \frac{\xi_{i+p+1} - \xi}{\xi_{i+p+1} - \xi_{i+1}} N_{i+1,p-1}(\xi) \end{aligned} \tag{11}$$

over the following knot vectors, in ξ, η and ζ directions, respectively:

$$\begin{aligned} \Xi &= \{\underbrace{0, \ldots, 0}_{p+1}, \xi_{p+1}, \ldots, \xi_{s_p-p-1}, \underbrace{1, \ldots, 1}_{p+1}\}, \quad \text{with} \quad s_p = n+p+1 \\ \mathcal{H} &= \{\underbrace{0, \ldots, 0}_{q+1}, \eta_{q+1}, \ldots, \eta_{s_q-q-1}, \underbrace{1, \ldots, 1}_{q+1}\}, \quad \text{with} \quad s_q = m+q+1 \\ \mathcal{Z} &= \{\underbrace{0, \ldots, 0}_{r+1}, \zeta_{r+1}, \ldots, \zeta_{s_r-r-1}, \underbrace{1, \ldots, 1}_{r+1}\}, \quad \text{with} \quad s_r = l+r+1 \end{aligned} \tag{12}$$

When knots are equally spaced in the parametric domain they are referred to as uniform. Otherwise, they are called non uniform. By changing the knot span lengths, more sample points can be used in regions where the curvature is high. A knot vector is considered as being open (or nonperiodic) when the first and last knots are defined $p+1$ times, implying that the first and last control points interpolate the geometry. In addition, when consecutive knots present the same value, knot spans of zero length are defined and knot multiplicity is obtained. The knot multiplicity is limited to the order of the basis function, when the basis function becomes interpolatory, i.e., when a knot value has multiplicity $p+1$ a subdivision is obtained. It is also important to notice that the support of each basis function over the knot spans is $p+1$.

Derivatives of the B-*spline* basis functions are represented in terms of B-*spline* lower order bases owing to the recursive definition of the basis functions. The derivative of the *i*-th basis function with respect to the parametric coordinate is defined as:

$$\frac{d}{d\xi} N_{i,p}(\xi) = \frac{p}{\xi_{i+p} - \xi_i} N_{i,p-1}(\xi) - \frac{p}{\xi_{i+p+1} - \xi_{i+1}} N_{i+1,p-1}(\xi) \tag{13}$$

For higher derivatives, the following generalization may be adopted:

$$\frac{d^k}{d\xi^k} N_{i,p}(\xi) = \frac{p}{\xi_{i+p} - \xi_i} \left(\frac{d^{k-1}}{d\xi^{k-1}} N_{i,p-1}(\xi) \right) - \frac{p}{\xi_{i+p+1} - \xi_{i+1}} \left(\frac{d^{k-1}}{d\xi^{k-1}} N_{i+1,p-1}(\xi) \right) \tag{14}$$

The derivatives of B-*spline* basis functions are defined over the same knot vector. Algorithms for numerical evaluation of derivatives of B-*spline* basis functions may be found in Piegl and Tiller (1997).

The most important properties related to B-spline may be summarized as follows:

- In the absence of repeated knots, continuous derivatives of order $p-1$ are maintained;
- The basis functions are nonnegative over the entire parametric domain;
- The basis functions constitute a partition of unity, that is: $\sum_{j=i-p}^{i} N_{j,p}(\xi) = 1 \; \forall \; \xi \in [\xi_i, \xi_{i+1})$;
- The number of continuous derivatives is decreased by k when a knot is repeated k times;
- The affine covariance property guarantees that any transformation on a B-*spline* curve is obtained applying the transformation directly to the control points.

Given $n+1$ basis functions $N_{i,p}$ of degree p and the corresponding control points $\mathbf{P}_i$, a B-*spline* curve may be described as:

$$\mathbf{C}(\xi) = \sum_{i=0}^{n} N_{i,p}(\xi)\,\mathbf{P}_i \tag{15}$$

where the knot vector (Ξ) is specified as expressed previously. B-*spline* surfaces are obtained considering a tensor product of univariate B-*spline* basis functions and a bi-dimensional net of control points $\mathbf{B}_{i,j}$, with $0 \leqslant i \leqslant n$ and $0 \leqslant j \leqslant m$, that is:

$$\mathbf{S}(\xi,\eta) = \sum_{i=0}^{n}\sum_{j=0}^{m} N_{i,p}(\xi)\,N_{j,q}(\eta)\,\mathbf{P}_{i,j} \tag{16}$$

where $N_{i,p}$ and $N_{j,q}$ are B-*spline* basis functions of degree p and q, respectively, and the knot vectors $(\Xi, \mathcal{H})$ are specified as expressed previously. B-*spline* solids are obtained analogously to B-*spline* surfaces, by considering a three-dimensional net of control points $B_{i,j,k}$, with $0 \leqslant i \leqslant n$ and $0 \leqslant j \leqslant m$ and $0 \leqslant k \leqslant l$, where $N_{i,p}$, $N_{j,q}$ and $N_{k,r}$ are B-*spline* basis functions of degree p, q and r, respectively and the knot vectors $(\Xi, \mathcal{H}, \mathcal{Z})$ are specified as expressed previously:

$$\mathbf{G}(\xi,\eta,\zeta) = \sum_{i=0}^{n}\sum_{j=0}^{m}\sum_{k=0}^{n} N_{k,r}(\xi)\,N_{j,q}(\eta)\,N_{k,r}(\zeta)\,\mathbf{P}_{i,j,k} \tag{17}$$

Geometrical entities can be also represented using rational polynomials, where conic sections such as circles and ellipses are exactly constructed taking into account projective transformations of piecewise quadratic curves (Roberts, 1965; Riesenfeld, 1981; Patterson, 1985). A rational function is defined as any function which can be written as the ratio of two polynomial functions. Homogeneous coordinates may be utilized to represent rational polynomials in a *n*-dimensional space by using a polynomials in *n+1*-dimensional homogeneous space. Homogeneous coordinates were proposed by Roberts (1965); Riesenfeld (1981). Computational algorithms in homogeneous coordinates are very efficient and they can be found in Piegl and Tiller (1997).

When the rational concept is applied to non uniform B-*spline*, Non Uniform Rational B-*spline* (NURBS) are obtained, which represent a significant improvement over standard B-*spline*, since complex objects cannot be exactly represented using simple polynomials. NURBS entities are then obtained by a projective transformation of B-*spline* entities.

Transformations are performed by projecting every point $(xw, yw, zw, w) = (X, Y, Z, W)$ belonging to the curve, surface or solid onto a hyperplane W = 1 through a line passing by the origin, i.e., the mapping is performed by $(x, y, z) = (\frac{X}{W}, \frac{Y}{W}, \frac{Z}{W})$ and this mapping generates the rational functions. The control points for NURBS are obtained by performing the same projective transformation to the control points of the B-*spline*, such that $\mathbb{R}^{d+1} \xrightarrow{\text{map}} \mathbb{R}^d$, where d is the euclidean space dimension (see Figure 1). The control points for NURBS curves are

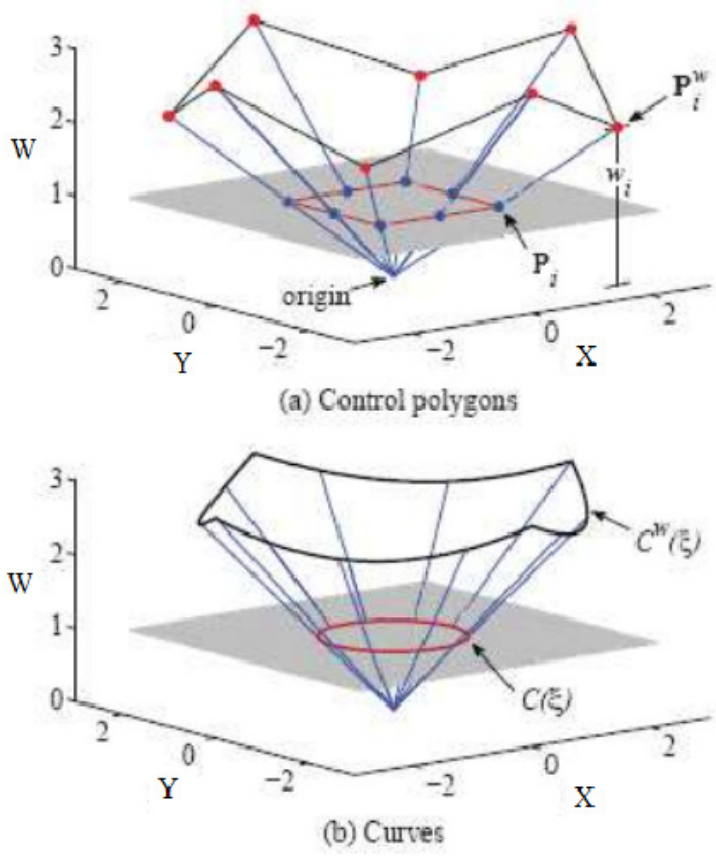

Figure 1: Curve representations using NURBS (Cottrell et al., 2009).

obtained by mapping, $\mathbf{P}^w \xrightarrow{\text{map}} \mathbf{P}$, using the following expression:

$$(\mathbf{P}_i)_j = \frac{(\mathbf{P}_i^w)_j}{w_i} \quad 1 \leqslant j \leqslant d; \qquad w_i = (\mathbf{P}_i^w)_{d+1} \tag{18}$$

where $(\mathbf{P}_i)_j$ is the *j*-th component of the vector of control points $\mathbf{P}_i$, w_i is referred to be the *i*-th weight and the $\mathbf{P}_i^w$ are associated to the projective control points. Dividing the projective control points by the weight is equivalent to applying the projective transformation to them.

The homogeneous concept allows an efficient approach to work with these entities, i.e., the

NURBS curve in homogeneous coordinates is defined as:

$$\mathbf{C}^w(\xi) = \sum_{i=0}^{n} N_{i,p}(\xi)\,\mathbf{P}_i^w \tag{19}$$

while the NURBS surface and solid in homogeneous coordinates are defined as

$$\mathbf{S}^w(\xi,\eta) = \sum_{i=0}^{n}\sum_{j=0}^{m} N_{i,p}(\xi)\,N_{j,q}(\eta)\,\mathbf{P}_{i,j}^w \tag{20}$$

and

$$\mathbf{G}^w(\xi,\eta,\zeta) = \sum_{i=0}^{n}\sum_{j=0}^{m}\sum_{k=0}^{n} N_{k,r}(\xi)\,N_{j,q}(\eta)\,N_{k,r}(\zeta)\,\mathbf{P}_{i,j,k}^w \tag{21}$$

where (p,q,r), $(n+1,m+1,l+1)$, (i,j,k), $(N_{i,p}(\xi), N_{j,q}(\eta), N_{k,r}(\zeta))$ are the degrees, the numbers of B-*spline* basis functions, the control points index, and the basis functions according to directions ξ, η and ζ, respectively. Note that the number of B-*spline* basis functions is identical to the number of control points. The control points in homogeneous coordinates are given in the following form:

- For curves $\mathbf{P}_i^w = (w_i x_i, w_i y_i, w_i z_i, w_i)$;
- For surfaces $\mathbf{P}_{i,j}^w = (w_{i,j} x_{i,j}, w_{i,j} y_{i,j}, w_{i,j} z_{i,j}, w_{i,j})$;
- For solids $\mathbf{P}_{i,j,k}^w = (w_{i,j,k} x_{i,j,k}, w_{i,j,k} y_{i,j,k}, w_{i,j,k} z_{i,j,k}, w_{i,j,k})$.

A curve $\mathbf{C}(\xi)$ is related to its projective curve $\mathbf{C}^w(\xi)$ by the following expression:

$$\left(\mathbf{C}(\xi)\right)_j = \frac{\left(\mathbf{C}^w(\xi)\right)_j}{W(\xi)} \quad 1 \leqslant j \leqslant d; \qquad W(\xi) = \sum_{i=0}^{n} N_{i,p}(\xi)\,w_i \tag{22}$$

where $W(\xi)$ is the weighting function and $N_{i,p}$ is the standard B-*spline* basis function. NURBS basis functions are finally defined as follows:

$$R_i^p(\xi) = \frac{N_{i,p}(\xi)\,w_i}{\sum_{\hat{i}=0}^{n} N_{\hat{i},p}(\xi)\,w_{\hat{i}}} \tag{23}$$

A NURBS curve of degree p is defined using Eq. (23) in conjunction with the control points defined by Eq. (18), that is:

$$\mathbf{C}(\xi) = \sum_{i=0}^{n} R_i^p(\xi)\,\mathbf{P}_i \tag{24}$$

Rational surfaces and solids are analogously defined considering tensor products of rational basis functions given, respectively, by

$$R_{i,j}^{p,q}(\xi,\eta) = \frac{N_{i,p}(\xi)\,N_{j,q}(\eta)\,w_{i,j}}{\sum_{\hat{i}=0}^{n}\sum_{\hat{j}=0}^{m} N_{\hat{i},p}(\xi)\,N_{\hat{j},q}(\eta)\,w_{\hat{i},\hat{j}}} \tag{25}$$

and

$$R^{p,q,r}_{i,j,k}(\xi,\eta,\zeta) = \frac{N_{i,p}(\xi)\, N_{j,q}(\eta)\, N_{k,r}(\zeta)\, w_{i,j,k}}{\sum_{\hat{i}=0}^{n}\sum_{\hat{j}=0}^{m}\sum_{\hat{k}=0}^{l} N_{\hat{i},p}(\xi)\, N_{\hat{j},q}(\eta)\, N_{\hat{k},r}(\zeta)\, w_{\hat{i},\hat{j},\hat{k}}} \tag{26}$$

If the weights are equal to one, then $R_{i,p} = N_{i,p}$. Hence, B-*splines* may be considered as a special case of NURBS.

Derivatives of NURBS basis functions are obtained according to the following expression:

$$\frac{d}{d\xi}R^p_i(\xi) = w_i \frac{W(\xi)\, N'_{i,p}(\xi) - W'(\xi)\, N_{i,p}(\xi)}{(W(\xi))^2} \tag{27}$$

where $N'_{i,p}(\xi) \overset{\text{def}}{=} \frac{d}{d\xi}N_{i,p}(\xi)$ and $W'(\xi) \overset{\text{def}}{=} \sum_{i=0}^{n} N_{i,p} w_i(\xi)$

For higher order derivatives, Piegl and Tiller (1997) suggest the following expression:

$$\frac{d^k}{d\xi^k}R^p_i(\xi) = \frac{A^{(k)}_i(\xi) - \sum_{j=1}^{k}\binom{k}{j} W^{(j)}(\xi)\, \frac{d^{(k-j)}}{d\xi^{(k-j)}}R^p_i(\xi)}{W(\xi)} \tag{28}$$

where $A^{(k)}_i = w_i \frac{d^k}{d\xi^k}N_{i,p}(\xi)$ (no sum on i); $W^{(k)}(\xi) = \frac{d^k}{d\xi^k}W(\xi)$. Additional information on NURBS may be found in Piegl and Tiller (1997); Espath (2009).

2.2 Fundamental concepts on IsoGeometric Analisys

Elements in Finite Element Analysis (FEA) are represented using the parent and physical domains, where geometry and degrees-of-freedom are defined in terms of their nodal values. In addition, finite element basis functions are usually interpolatory, which may assume positive as well as negative values (see, for instance, Bathe (1995)). On the other hand, Isogeometric Analysis utilizes NURBS basis functions and two concepts about numerical meshes can be identified: the control and physical meshes. Control points are defined in order to control the geometry and they do not conform to the actual geometry. The control mesh looks like a finite element mesh constructed with multilinear elements. Geometry and degrees-of-freedom are represented in terms of their respective values defined at the control points.

Two definitions can be also observed for the physical mesh: the patch and knot meshes. Patches may be considered as macro-elements, which have representations in the parent and physical domains. Each patch can be decomposed into knot spans and Knots may be points, curves and surfaces in one-, two- and three-dimensional topologies, respectively. Knots define knot spans and element domains, where basis functions are smooth (C^∞). Across the knots, basis functions are C^{p-m} continuous, where p is the polynomial degree and m is the multiplicity of the knot. Knot spans also define the domain where numerical quadrature takes place, being represented in the parent and physical domains. Another important concept is related to the index space of a patch, which identifies each knot and determinates knots having multiplicity greater than one. In Figure 2, a simple case of surface parameterization with NURBS is shown.

The isoparametric concept is very important for Isogeometric Analysis, since the basis functions utilized to exactly represent the geometrical model are also employed to approximate the

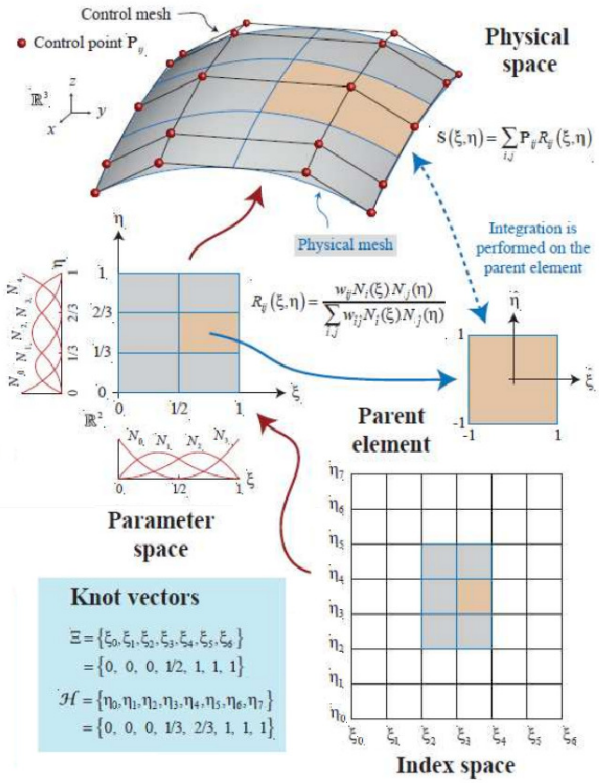

Figure 2: General concepts involving Isogeometric Analysis (Cottrell et al., 2009).

solution space. On the other hand, when the isoparametric concept is applied to the Finite Element Analysis (FEA), the basis adopted to approximate the unknown solution field is then used to approximate the geometrical model.

The maximum level of continuity across an element boundary, for example, is determined by continuity of the basis across the corresponding knot span. If the level of refinement is insufficient, the basis must be refined. However, it is important to notice that the refinement procedure maintains both, the geometry and the parameterization, unchanged.

Any function is represented over the entire parametric domain by using the following expression

$$u\left(\xi\right) \overset{\text{def}}{=} \sum_{i=1}^{n_{np}} N_a\left(\xi\right) d_a \tag{29}$$

where n_{np} is the total number of control points in the control mesh, N_a is the NURBS basis function associated to control point a, with $a \in [1, n_{np}]$, considering that coordinates and unknowns are defined in the vector of control variables d_a.

2.3 A numerical model for linear and geometrically nonlinear elasticity

Problems on Elastostatics may be formulated as a special case of the first Cauchy's law of motion, which is usually referred to as the equilibrium equation. In addition, mass and energy conservation must be enforced over the volume enclosing the body (see Malvern (1969)). Considering a classical Lagrangian kinematical description in the Cartesian coordinate system and in the absence of temperature changes and inertial forces, the conservation equations are

reduced to the following expressions:

$$\begin{aligned} \int_{\Omega_0} \rho\left(\mathbf{X}, t_0\right) d\Omega &= \int_{\Omega} \rho\left(\mathbf{x}, t\right) d\Omega \\ \text{div}\, \boldsymbol{\sigma} + \mathbf{b} &= \mathbf{0} \quad \text{in} \quad \Omega \end{aligned} \tag{30}$$

where div $\boldsymbol{\sigma} = \nabla^T \boldsymbol{\sigma}$ and ∇ is the nabla differential operator, $\mathbf{X}$ and $\mathbf{x}$ are vectors containing components of the material (X_i) and spatial (x_i) coordinates in the Cartesian coordinate system, respectively, t represents time, ρ is the specific mass, $\mathbf{b}$ is the body force vector and $\boldsymbol{\sigma}$ contains components of the Cauchy stress tensor. It is important to notice that the equilibrium equation, which is derived from the Cauchy's equation of motion, is defined taking into account the current deformed configuration of the body (Ω).

When infinitesimal displacements and rotations are observed, the geometrical linear approach can be utilized, where the undeformed configuration of the body is taken as reference throughout the analysis. In addition, the Cauchy stress tensor and the infinitesimal strain tensor are adopted in order to describe the stress-strain relation. On the other hand, when displacements and rotations are large, a special treatment must be considered in order to obtain accurate results for the strain field.

In the present model, geometrically nonlinear problems are analyzed considering a corotational formulation for the kinematical description of the continuum, where stress and strain are described according to a coordinate system locally attached to every element of the physical mesh. A linear hypoelastic constitutive model restricted to small strains is adopted in order to relate strain and stress measures in the elastic regime, which may be written as $\boldsymbol{\sigma} = \mathbf{D}^e \boldsymbol{\epsilon}$, where $\boldsymbol{\epsilon}$ contains components of the strain tensor and $\mathbf{D}^e$ is the constitutive matrix containing components of a fourth order tensor. Stress updates are performed by using the Truesdell rate, which may be written as follows:

$$\dot{\boldsymbol{\sigma}}^{tr} = \dot{\boldsymbol{\sigma}} - \mathbf{L}\boldsymbol{\sigma} - \boldsymbol{\sigma}\mathbf{L}^{\mathbf{T}} + \boldsymbol{\sigma} tr\left(\boldsymbol{\epsilon}\right); \qquad \mathbf{L} = \dot{\boldsymbol{\epsilon}} + \dot{\boldsymbol{\omega}} \tag{31}$$

where $\dot{\boldsymbol{\epsilon}}$ and $\dot{\boldsymbol{\omega}}$ are the strain and spin tensors, respectively. Increments of the strain rate and spin rate tensor components are evaluated employing the mid-point integration within the increment interval $[t_n, t_{n+1}]$, that is:

$$\int_{t_n}^{t_{n+1}} \mathbf{L} d\tau = \Delta\boldsymbol{\epsilon} + \Delta\boldsymbol{\omega} = \frac{1}{2}\left[\frac{\partial \Delta \mathbf{u}^{def}}{\partial \hat{x}_{n+1/2}} + \left(\frac{\partial \Delta \mathbf{u}^{def}}{\partial \hat{x}_{n+1/2}}\right)^T\right] + \frac{1}{2}\left[\frac{\partial \Delta \mathbf{u}^{def}}{\partial \hat{x}_{n+1/2}} - \left(\frac{\partial \Delta \mathbf{u}^{def}}{\partial \hat{x}_{n+1/2}}\right)^T\right] \tag{32}$$

with

$$\Delta \hat{\mathbf{u}}^{def} = \mathbf{R}_{n+1/2}^T \Delta \mathbf{u}^{def} = \hat{\mathbf{x}}_{n+1} - \hat{\mathbf{x}}_n \tag{33}$$

where $\Delta \mathbf{u}^{def}$ is the deformation part of the total displacement field and $\hat{\mathbf{x}}_n$ and $\hat{\mathbf{x}}_{n+1}$ are body configurations defined in the corotational coordinate system at $t = t_n$ and $t = t_{n+1}$, both being expressed as follows:

$$\hat{\mathbf{x}}_n = \mathbf{R}_n^T \mathbf{x}_n; \qquad \hat{\mathbf{x}}_{n+1} = \mathbf{R}_{n+1}^T \mathbf{x}_{n+1} \tag{34}$$

where $\mathbf{R}_n$, $\mathbf{R}_{n+1/2}$ and $\mathbf{R}_{n+1}$ are orthogonal tensor performing objective transformations between the global coordinate system to the corresponding corotational systems, which are defined at $t = t_n$, $t = t_{n+1/2}$ and $t = t_{n+1}$, respectively. The rotation matrices are evaluated in this

work considering the classical polar decomposition based on the left stretch tensor. Additional information on the corotational formulation utilized in the present paper may be found in Braun and Awruch (2008).

Applying the Bubnov-Galerkin weighted residual method in conjunction with the Green-Gauss theorem over the momentum equation (given in Eq. (30)), the following expression is obtained:

$$\int_{\Omega} (\nabla \delta \mathbf{u})^T \boldsymbol{\sigma} d\Omega = \int_{\Omega} \delta \mathbf{u}^T \mathbf{b} d\Omega + \int_{\Gamma} \delta \mathbf{u}^T \mathbf{t} d\Gamma \tag{35}$$

where $\mathbf{t}$ is the surface traction vector and Ω and Γ are, respectively, volume and boundary surface referred to the physical space where the problem takes place. In order to define the element concept in the context of Isogeometric Analysis, geometry as well as displacements and displacement variations are represented with the following expressions:

$$\mathbf{x}(\boldsymbol{\xi}) = \sum_{a=1}^{n_{np}} R_a(\boldsymbol{\xi}) \mathbf{x}_a; \qquad \mathbf{u}(\boldsymbol{\xi}) = \sum_{a=1}^{n_{np}} R_a(\boldsymbol{\xi}) \mathbf{u}_a; \qquad \delta \mathbf{u}(\boldsymbol{\xi}) = \sum_{a=1}^{n_{np}} R_a(\boldsymbol{\xi}) \delta \mathbf{u}_a \tag{36}$$

where R_a is the NURBS basis function related to control point a, which is defined as function of the vector of parametric coordinates $\boldsymbol{\xi} = \{\xi, \eta, \zeta\}$, and n_{np} is the number of global basis functions. Knot vectors corresponding to the different directions in the parametric space must be specified defining the non-zero knot spans where elements are then identified. Notice that unlike finite element models, where geometry and solution fields are approximated at element level, the respective approximations given by Isogeometric Analysis (see Eq. (36)) are valid for the entire parametric space, although NURBS basis functions present localized support. Some basis functions and their respective control points may belong to different elements simultaneously, since the basis functions are extended over $p+1$ knot spans, where p is the polynomial degree. Consequently, Eq. (35) can be rewritten as:

$$\sum_{e=1}^{n_{el}} \left(\int_{\Omega_e} (\nabla \delta \mathbf{u})^T \boldsymbol{\sigma} d\Omega_e \right) = \sum_{e=1}^{n_{el}} \left(\int_{\Omega_e} \delta \mathbf{u}^T \mathbf{b} d\Omega_e + \int_{\Gamma_e} \delta \mathbf{u}^T \mathbf{t} d\Gamma_e \right) \tag{37}$$

where Ω_e and Γ_e are, respectively, volume and boundary surface corresponding to element e in the physical mesh. Considering $n+1$, $m+1$ and $l+1$ as the number of basis function corresponding to the parametric directions ξ, η and ζ, respectively, and their respective polynomial degree defined by p, q and r, element e is defined by determining the indices at which the corresponding non-zero knot span begins in the index space (see Figure 2), that is:

$$e \in [\xi_i, \xi_{i+1}] \times [\eta_i, \eta_{i+1}] \times [\zeta_i, \zeta_{i+1}] \tag{38}$$

where $p+1 \leqslant i \leqslant n$, $q+1 \leqslant j \leqslant m$ and $r+1 \leqslant k \leqslant l$. The total number of elements in which the spatial field is discretized in the parametric domain is defined as:

$$n_{el} = (n-p+1) \cdot (m-q+1) \cdot (l-r+1) \tag{39}$$

The index space also determines the NURBS coordinates, which are related to the indices of a knot that define a knot vertex in the physical mesh. Consequently, by examining the index

space, it is possible to determine exactly which basis functions have support in element e with the following expressions:

$$\begin{array}{lll} N_\alpha(\xi) \text{ over } \Xi & \text{have support for } \alpha \in [i-p, i] \\ N_\beta(\eta) \text{ over } \mathcal{H} & \text{have support for } \beta \in [j-q, j] \\ N_\gamma(\zeta) \text{ over } \mathcal{Z} & \text{have support for } \gamma \in [k-r, k] \end{array} \tag{40}$$

NURBS coordinates are also utilized to specify the knot at which the support of a basis function begins. Taking into account these NURBS coordinates, a global numbering scheme for trivariate basis functions and the respective control points may be formulated as follows:

$$\tilde{N}_A(\xi,\eta,\zeta) = N_i(\xi) N_j(\eta) N_k(\zeta) \quad (i,j,k) \in [0,n] \times [0,m] \times [0,l] \tag{41}$$

where

$$\begin{aligned} A &= (m+1)(n+1)k + (n+1)j + i + 1 \\ (\xi,\eta,\zeta) &\in [\xi_i, \xi_{i+p+1}] \times [\eta_j, \eta_{j+q+1}] \times [\zeta_k, \zeta_{k+r+1}] \end{aligned} \tag{42}$$

A numbering scheme to assign element numbers may be defined with:

$$e = (k-r)(m-q+1)(n-p+1) + (j-q)(n-p+1) + (i-p+1) \tag{43}$$

The total number of control points and their respective NURBS basis functions are given observing the number of components in the knot vectors and the polynomial order defined for the basis functions. Hence, refinements can be obtained by including components in the knot vectors, which leads to increasing the number of control points or the polynomial degree. In the present work, only single patches and open knot vectors are considered.

In order to establish a local framework for assembling the global matrix formulation in accordance with the FEM practice, the local dimensions of matrices and vectors are first specified taking into account that the number of basis functions acting locally on an element is determined by:

$$n_{en} = (p+1)(q+1)(r+1) \tag{44}$$

A local numbering scheme for identifying the basis functions is then formulated, which is based on the NURBS coordinates utilized to determine the location of a given element. With the element number determined, local function number 1 is assigned to the global basis function with NURBS coordinates (i,j,k), which define the element position in the index space. The remaining global basis functions of the present element are then enumerated by assigning numbers from 2 up to n_{en}, where a descendent sequence over the global basis functions is considered. These local numbers are assigned working backwards in ξ direction until $A-p$ is obtained, with A determined by Eq. (42). The parametric directions η and ζ are then run using the same descendent characteristic. Since some of the global basis functions are extended over different elements, the corresponding control points determine element connectivities, which are utilized to assemble the global system of governing equations in matrix form. Figure 3 illustrates the process of local numbering for a simple case

By substituting the NURBS approximation related to the displacement field, given by Eq. (36), into the constitutive equation, an element level approximation for the stress-strain relation is obtained, where the strain components are given by:

$$\boldsymbol{\epsilon} = \mathbf{B}\mathbf{u} \tag{45}$$

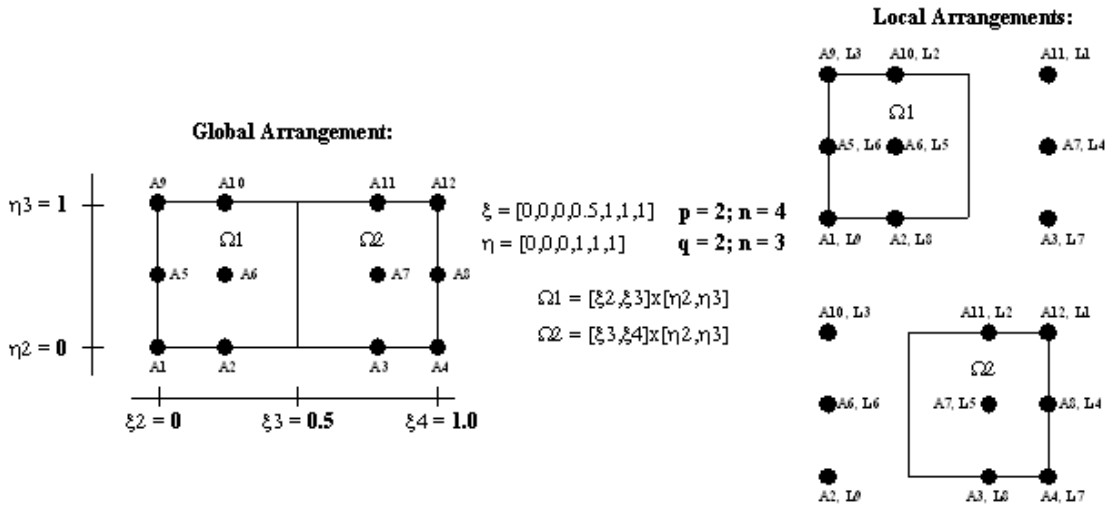

Figure 3: The local numbering scheme.

being $\mathbf{B}$ the gradient matrix. For geometrically nonlinear analysis, $\mathbf{B}$ must be evaluated considering the current configuration of the body in the corotational coordinate system.

Introducing the expansions of displacements components and their corresponding variations, given by Eq. (36), and the relationship given in Eq. (45) into Eq. (37), a matrix equation representing a system of linear algebraic equations is obtained for the equilibrium equation, which may be expressed as:

$$\sum_{e=1}^{n_{el}} \mathbf{K}^e \mathbf{u} = \sum_{e=1}^{n_{el}} \mathbf{f}^e \tag{46}$$

where $\mathbf{K}^e$ is the element stiffness matrix and $\mathbf{F}^e$ is the force vector at element level. The matrix and vector dimensions associated to $\mathbf{K}^e$ and $\mathbf{F}^e$ are specified as $(n_{eq} \cdot n_{eq} \cdot n_{eq})$ and (n_{eq}), respectively, where $n_{eq} = n_{en} \cdot n_{dof}$, with n_{dof} denoting the number of degrees of freedom at the control points level. The summation symbol indicates the assembling procedure to evaluate the global system of equations, considering the element contributions given according to connectivity relations established previously. The global stiffness matrix is always sparse because the support of each basis function is highly localized. In the geometrically nonlinear regime, the momentum equation (Eq. (35)) must be iteratively satisfied using the incremental approach (see Bathe (1995)), since internal forces are given now as functions of the current configuration of the body. The nonlinear equilibrium equation is obtained employing a linearization procedure given by the Newton-Raphson method, where the residual vector is submitted to a Taylor series expansion within the increment interval $[t, t + \Delta t]$. Eq. (46) is then rewritten as follows:

$$\sum_{e=1}^{n_{el}} \mathbf{K}^e_{tan}\left(\mathbf{u}^e\right) \mathbf{u} = \sum_{e=1}^{n_{el}} \mathbf{f}^e - \sum_{e=1}^{n_{el}} \mathbf{f}^e_{int}\left(\mathbf{u}^e\right) \tag{47}$$

where $\mathbf{K}^e_{tan}$ is the tangent stiffness matrix. At each iterative step, the tangent stiffness matrix and the internal force vector are initially evaluated in the corotational coordinate system with the following expressions:

$$\hat{\mathbf{K}}^e_{tan} = \int_{\hat{\Omega}^e} \mathbf{B}^T \left(\mathbf{D} + \hat{\mathbf{D}}\right) \mathbf{B} d\hat{\Omega}^e; \quad \hat{\mathbf{f}}^e_{int} = \int_{\hat{\Omega}^e} \mathbf{B}^T \boldsymbol{\sigma} d\hat{\Omega}^e \tag{48}$$

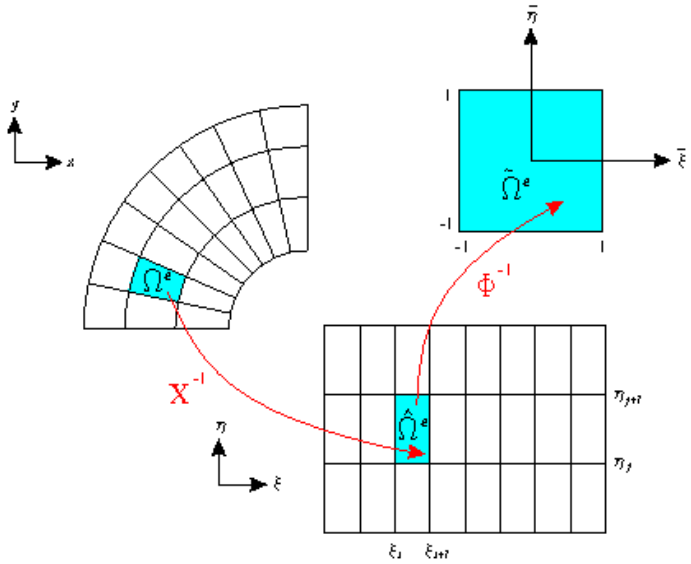

Figure 4: The physical, parametric and parent spaces utilized in the numerical integration of the stiffness matrix (Cottrell et al., 2009).

where $\hat{\Omega}^e$ is referenced to the current configuration of element e in the corotational coordinate system, $\hat{\mathbf{D}}$ and $\boldsymbol{\sigma}$ are stress tensors related to the Truesdell rate tensor and the corotational Cauchy stress tensor, respectively, with both evaluated in the corotational coordinate system. In order to solve the system of nonlinear equilibrium equations, the tangent stiffness matrix and the internal force vector must be obtained in the global coordinate system through an objective transformation from the corotational system, that is:

$$\mathbf{K}^e_{tan} = \mathbf{R}\hat{\mathbf{K}}^e_{tan}\mathbf{R}^T; \quad \mathbf{f}^e_{int} = \mathbf{R}\hat{\mathbf{f}}^e_{int} \tag{49}$$

The numerical integration associated to the evaluation of the element stiffness matrix is performed using Gaussian quadrature. Integrals defining the matrix terms, which are initially defined in the physical space, are transferred to the parametric space and then to the parent space, where the numerical integration is actually performed. Considering that coordinates in the physical, parametric and parent spaces are denoted by $\mathbf{x}$, $\hat{\boldsymbol{\xi}}$ and $\tilde{\boldsymbol{\xi}}$, respectively, elements can be similarly denoted as Ω^e , $\hat{\Omega}^e$ and $\tilde{\Omega}^e$ in the physical, parametric and parent domains (see Figure 4). The transformation from the physical space to the parent space, where Gaussian quadrature is carried out, is achieved by using a composition of two consecutive transformations: the physical space is transferred first to the parametric space through a geometrical mapping and then to the parent space through a second mapping, which is affine. Spatial derivatives of basis functions with respect to Cartesian coordinates are substituted by the corresponding derivatives with respect to the parametric coordinates as follows:

$$\frac{\partial R}{\partial x_i} = \frac{\partial R}{\partial \hat{\xi}_j}\frac{\partial \hat{\xi}_j}{\partial x_i} \tag{50}$$

where $(\hat{\xi}_1, \hat{\xi}_2, \hat{\xi}_3) = (\hat{\xi}_1, \hat{\eta}_2, \hat{\zeta}_3)$ and the second term on the right-hand side of Eq. (50) represents the inverse of the Jacobian matrix. Since the numerical integration is performed in the parent domain, the Jacobian determinant is evaluated with:

$$J = \left|\frac{\partial x_i}{\partial \tilde{\xi}_j}\right| = \left|\frac{\partial x_i}{\partial \hat{\xi}_k}\frac{\partial \hat{\xi}_k}{\partial \tilde{\xi}_j}\right| \tag{51}$$

where $(\tilde{\xi}_1, \tilde{\xi}_2, \tilde{\xi}_3) = (\tilde{\xi}_1, \tilde{\eta}_2, \tilde{\zeta}_3)$. The parametric coordinates $(\hat{\xi}_1, \hat{\eta}_2, \hat{\zeta}_3)$ related to the quadrature points defined in the parent domain $(\tilde{\xi}_1, \tilde{\eta}_2, \tilde{\zeta}_3)$ can be obtained considering the NURBS coordinates (i, j, k) associated to element $e \in [\xi_i, \xi_{i+1}] \times [\eta_j, \eta_{j+1}] \times [\zeta_k, \zeta_{k+1}]$, that is:

$$\begin{aligned} \hat{\xi} &= \hat{\xi}_i + (\tilde{\xi} + 1)\frac{\hat{\xi}_{i+1} - \hat{\xi}_i}{2} \\ \hat{\eta} &= \hat{\eta}_i + (\tilde{\eta} + 1)\frac{\hat{\eta}_{i+1} - \hat{\eta}_i}{2} \\ \hat{\zeta} &= \hat{\zeta}_i + (\tilde{\zeta} + 1)\frac{\hat{\zeta}_{i+1} - \hat{\zeta}_i}{2} \end{aligned} \tag{52}$$

Although the present integration scheme is only approximated, it is important to notice that the classical Gaussian quadrature over rational functions is an approximation as well.

When a numerical model based on Isogeometric Analysis is formulated with Bubnov-Galerkin method and NURBS basis functions, homogeneous boundary conditions are exactly enforced by setting the corresponding control variables (basis functions) as zero. A trivial procedure for imposition of essential boundary conditions is then obtained, which is similar to that utilized by finite element models. In the present model, the Kroenecker delta property of the NURBS basis functions can be applied on the displacement field as follows:

$$\mathbf{u}\left(\mathbf{x}_b\right) = \sum_{a=1}^{n_{np}} R_a\left(\boldsymbol{\xi}_b\right)\mathbf{u}_a = 0 \quad \text{with} \quad R_a\left(\mathbf{x}_b\right) = \delta_{ab} \tag{53}$$

where vector $\mathbf{x}_b$ specifies Cartesian coordinates of control points with parametric coordinates defined by $\boldsymbol{\xi}_b$, which are located at boundary knots with essential boundary conditions.

Unfortunately, for general inhomogeneous essential boundary conditions, significant errors may be obtained if these boundary conditions are applied directly to the control variables. Unlike FEA, where nodal points are located on the boundary surfaces, Isogeometric Analysis is usually carried out considering control points located outside the physical boundary surfaces. In addition, it is important to notice that NURBS basis functions are not interpolatory functions. For additional information on this subject, readers are addressed to a recent work presented by Wang and Xuan (2010).

2.4 Numerical applications

In this section two examples of elastic linear structural analysis and one example of an elastic geometrically nonlinear structural analysis are presented. The first example is a simply supported plate (Dirichlet boundary conditions are applied in the boundary of the middle surface of the solid) with an uniform normal load applied over the whole middle surface. The second example is known as the pinched cylinder problem. The pinched cylinder is subjected to equal and opposite concentrated forces at its midspan. At the ends, where structure is supported by rigid diaphragms the Dirichlet boundary conditions are applied. Only one octant of the cylinder is modeled. The nonlinear example is performed using a cantilever beam which is subjected to a constant bending moment. The moment is chosen such that a tip rotation of 2π rad is expected, i.e., the straight beam shall be bent to a circle.

2.4.1 Linear elastic plate

The simply supported plate is modeled as a solid and is analized using 3×3 elements in its surface and 2 elements through the thickness. In the plate surface the basis is chosen as a

quintic-NURBS, and through the thickness three cases are tested, linear-, cubic- and quintic-NURBS.

The plate (Figure 5) with a thickness equal to 0.1 and an area of 10×10 is submitted to an uniform load equivalent to 500. The material properties are: $E = 2.1 \cdot 10^{11}$ and $\nu = 0.3$.

The geometry is presented in Figure 5. Result of displacement is shown in 6a and deformed

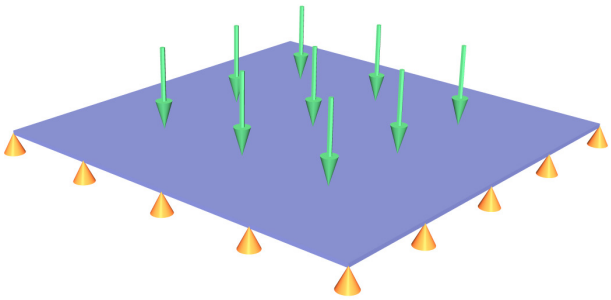

Figure 5: Geometry.

plate for one half of geometry is shown in 6b. The analytical solution for this problem has

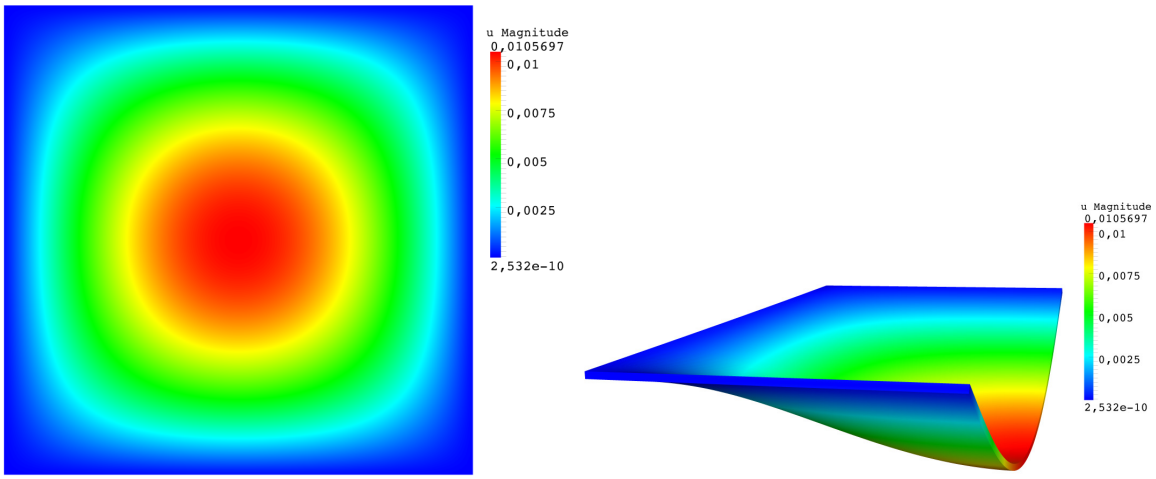

(a) Displacement (b) Half deformed plate

Figure 6: Plate simply supported.

a maximal displacement equal to 0.010556. In this example the maximal displacement using Isogeometric Analysis is 0.010569. Although the mesh used has a poor quality, for analyses carried out with cubic- and quintic-NURBS through the thickness the response is satisfactory. In these cases results are indistinguishable. For linear-NURBS through the thickness unacceptable results were obtained, with an error of 5% approximately. Using a more fine discretization, 16×16 elements in the surface, this error is reduced to 2.5%.

2.4.2 Linear elastic shell

A pinched cylindrical shell mounted on rigid end diaphragms was modeled as a solid and it is analized using 16×16 elements in its surface and 2 elements through the thickness. The pinched cylinder is subjected to equal and opposite concentrated forces at its midspan, equal to 1.0, (see Figure 7a).

The shell (Figure 7a) has a thickness equal to 3.0, being the radius equal to 300 and the length equal to 600. The material properties are: $E = 3.0 \cdot 10^6$ and $\nu = 0.3$. The maximal difference

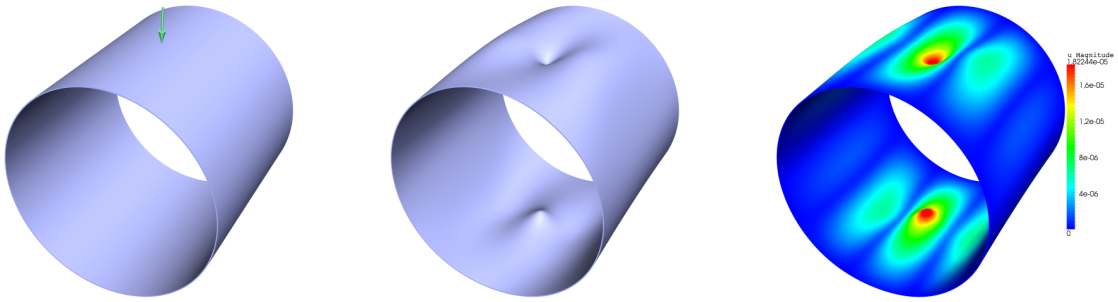

(a) Undeformed shell (b) Deformed shell (c) Displacement

Figure 7: Pinched cylinder.

obtained in the displacement (see Figure 7c) when compared with the analytical solution (see Cottrell et al. (2009)) is 0.1%. To obtain this result, the necessary mesh is at least formed by 16×16 elements. These simulations have been carried out for cubic- and quintic-NURBS through the thickness and the results are practically the same. However, results produced by linear-NURBS through the thickness are unacceptable for this mesh, 16×16.

2.4.3 Geometrically nonlinear elastic beam

A tip rotation of 2π rad is obtained for a cantilever beam under a tip bending moment $M = \dfrac{2\pi EI}{L}$, where E is Young's modulus and I is the moment of inertia. Since there are no rotational degrees of freedom, the moment is modeled by pairs of path forces (see Figure 8).

The beam has a the thickness equal to 0.1, the width is equal to 1.0 and the length is equal to 10. The material properties are: $E = 1.2 \cdot 10^5$ and $\nu = 0.0$. Results are presented in Figure 9, which show the geometries and displacements when the moment is increased step-by-step. The geometries correspond to 0%, 25%, 50%, 75% and 100% of the total moment. The load history is shown in Figure 10, where dots are the exact solution and the continuous lines was obtained with the corotational approach. These curves are the vertical and horizontal displacement, following sinusoidal functions. Two meshes were analized: 16 quintic-NURBS elements in length direction, 1 linear-NURBS through the thickness and in the width direction; the second mesh is slightly different, having 32 quintic-NURBS elements in length direction. Results for displacements, shown in Figure 10, are obtained with the second mesh. However, the first mesh yields results with an error which is less than 2.5%.

3 CONCLUSIONS

Some tests were performed in this work for linear and geometrically nonlinear structures, and good results were obtained. For the elastic linear structures excellent results were obtained with quintic-NURBS in the structural surface (even for very poor meshes), although it was necessary to use at least cubic-NURBS through the thickness. When linear-NURBS are used through the thicknessrelatively high errors occur. The geometrically nonlinear problem gives

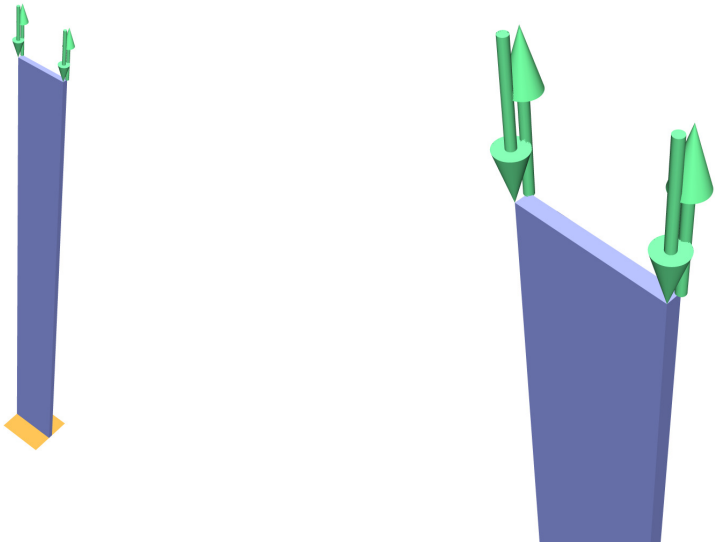

(a) Geometry and boundary conditions (b) Moment as a two pair of path forces

Figure 8: Beam bent to a circle.

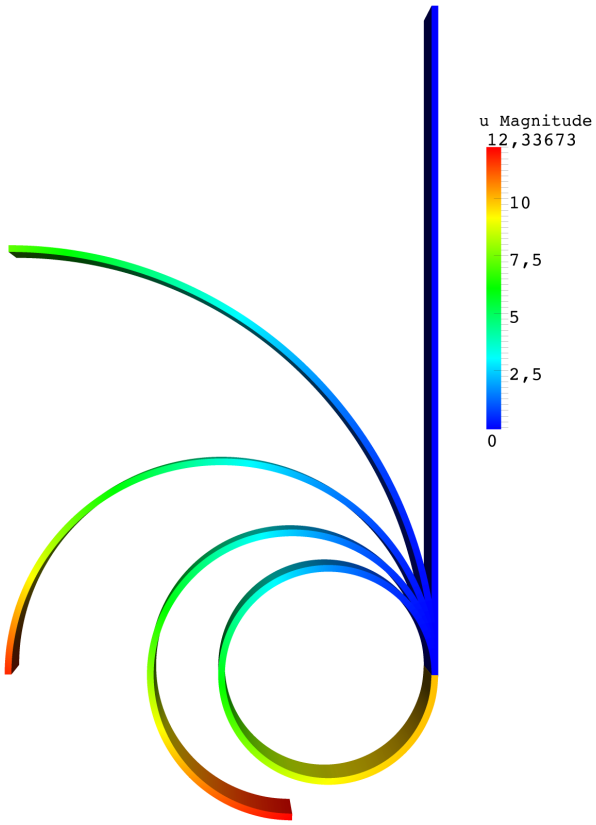

Figure 9: Circle beam.

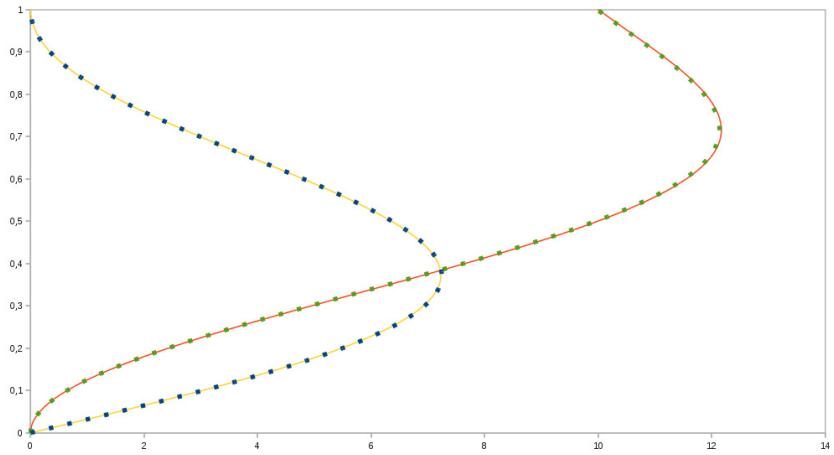

Figure 10: Load history (Vertical and Horizontal displacement vs. load).

the same results when compared with analytical solution. In this case, it is not necessary to use cubic-NURBS, or higher degree, through the thickness. Results were indistinguishable for any degree of NURBS through the thickness, then results presented for this example were obtained for linear-NURBS through the thickness

Finally, aims achieved in this work are listed below:

- Introduce basic concepts of NURBS and Isogeometric analysis;
- The shells, plates and beams could be easily modeled as solids, in displacement approach;
- An accurate kinematic description, using a corotational approach, was developed based on polar decomposition.

4 ACKNOWLEDGMENTS

The authors thank to CAPES and CNPq for their financial support; and thank to CESUP (UFRGS Supercomputing Center).

REFERENCES

Bathe K.J. *Finite Element Procedures*. Prentice Hall, 2th edition, 1995.

Bazilevs Y., Calo V., Cottrell J., Hughes T., Reali A., and Scovazzi G. Variational multiscale residual-based turbulenve modeling for large eddy simulation of incompressible flows. *Computer Methods in Applied Mechanics and Engineering*, Vol. 197:173–201, 2007.

Bernstein S.N. Démonstration du théorème de weierstrass fondée sûr le calcul dês probabilités. *Commun. Soc. Math*, Vol. 12(2):1–2, 1912.

Braun A. and Awruch A. Geometrically non-linear analysis in elastodynamics using the eight-node finite element with one-point quadrature and the generalized-α method. *Latin American Journal of Solids and Structures*, Vol. 5:17–45, 2008.

Bézier P.E. Définition numérique des courbes et surfâces i. *Automatisme*, Vol. XI:625–632, 1966.

Bézier P.E. Définition numérique des courbes et surfâces ii. *Automatisme*, Vol. XII:17–21, 1967.

Bézier P.E. *Numerical Control: Mathematics and applications*. John Wiley, New York, 1972.

Cottrell J., Hughes T., and Bazilevs Y. *Finite Element Procedures*. Wiley, 2009.

Cottrell J., Reali A., Bazilevs Y., and Hughes T. Isogeometric analysis of structural vibrations. *Computer Methods in Applied Mechanics and Engineering*, Vol. 195:5257–5296, 2006.

Cox M.G. The numerical evaluation of b-spline. *Inst. Math. Applic.*, Vol. 10(1):134–149, 1972.

deBoor C. On calculating with b-spline. *Approx. theory*, Vol. 6(1):50–72, 1972.

DeCasteljau P. Outillages méthodes calcul. Tecnical report, A. Citröen, Paris, FR, 1959.

Elguedj T., Bazilevs, Y., Calo V., and Hughes T. B and f projection methods for nearly incompressible linear and non-linear elasticity and plasticity using high-order nurbs elements. *Computer Methods in Applied Mechanics and Engineering*, Vol. 197:2732–2762, 2008.

Elguedj T., Bazilevs Y., Calo V., and Hughes T. Isogeometric analysis: Cad, finite elements, nurbs, exact geometry and mesh refinement. *Computer Methods in Applied Mechanics and Engineering*, Vol. 194:4135–4195, 2005.

Espath L.F.R. *Otimização de formas de cascas via deformação livre de forma baseado em NURBS*. Master's Thesis, PPGEC/UFRGS, 2009.

Malvern L. *Introduction to the Mechanics of a Continuous Medium*. Prentice Hall, 1969.

Patterson R.R. Projective transformations of the parameter of a bernstein-bézier curve. *ACM TOG*, Vol. 4(4):276–290, 1985.

Piegl L.A. and Tiller W. *The Nurbs Book*. Springer, 2th edition, 1997.

Riesenfeld R.F. Homogeneous coordinates and projective planes in computer graphics. *IEEE Comput. Graph. and Appli.*, Vol. 1(1):50–55, 1981.

Roberts D.F. Homogeneous matrix representation and manipulation of n-dimensional constructs. Tecnical report ms-1405, Lincoln Laboratory, MIT, Cambridge, MA, 1965.

Wang D. and Xuan J. An improved nurbs-based isogeometric analysis with enhanced treatment of essential boundary conditions. *Computer Methods in Applied Mechanics and Engineering*, Vol. 199:2425–2436, 2010.